ARTICLES

Ideal glass transitions for hard ellipsoids

M. Letz, R. Schilling, and A. Latz

Johannes-Gutenberg-Universität Mainz, D-55099 Mainz, Germany

(Received 7 February 2000; revised manuscript received 12 April 2000)

For hard ellipsoids of revolution we calculate the phase diagram for the idealized glass transition. Our equations cover the glass physics in the full phase space, for all packing fractions and all aspect ratios X_0. With increasing aspect ratio we find the idealized glass transition to become primarily driven by orientational degrees of freedom. For needlelike or platelike systems the transition is strongly influenced by a precursor of a nematic instability. We obtain three types of glass transition line. The first one ($\phi_c^{(B)}$) corresponds to the conventional glass transition for spherical particles which is driven by the cage effect. At the second one ($\phi_c^{(B')}$), which occurs for rather nonspherical particles, a glass phase is formed that consists of domains. Within each domain there is a nematic order where the center of mass motion is quasiergodic, whereas the interdomain orientations build an orientational glass. The third glass transition line ($\phi_c^{(A)}$) occurs for nearly spherical ellipsoids where the orientational degrees of freedom with odd parity, e.g., 180° flips, freeze independently from the positions.

PACS number(s): 64.70.Pf, 61.20.Gy, 61.30.Cz, 61.25.Em

I. INTRODUCTION

The dynamics of a molecular system that is supercooled toward the glass transition shows a variety of phenomena related to the nontrivial interplay between orientational and translational degrees of freedom caused, e.g., by steric hindrance. In thermodynamic equilibrium molecular systems already show, compared to simple liquids, a variety of different physical behavior. At low enough densities (or high enough temperatures) they form an isotropic liquid. On increasing the density they can undergo a transition into a crystal or several different liquid crystalline phases (like, e.g., a nematic phase). A crucial part of the interaction that causes these phenomena is given by the shape of the molecules. Therefore one may also expect different characteristic features for the glass transition in such systems.

A model system that allows one to study the translation-orientation interplay is a system of *N hard ellipsoids of revolution* in a box of volume V. The fluid of ellipsoids is characterized by two parameters: the aspect ratio $X_0 = b/a$ relating b and a, the major and minor axes of the ellipsoids, and the packing fraction ϕ, which is related to the number density $\rho = N/V$ by $\phi = \pi X_0 \rho / 6$.

In this work we start from a theory of liquids. We demonstrate that a *single* set of equations allows us to describe the glassy behavior for almost spherical particles up to large aspect ratios where prenematic order becomes crucial. The choice of the model system has also been motivated by the successful application of the ideal mode-coupling theory (MCT) for simple liquids [1], particularly to neutral colloidal suspensions. MCT gives a closed set of equations for the intermediate scattering function $S(\mathbf{q},t)$. Comparison between experimental [2] and MCT results [1,3] has shown good agreement for colloidal systems which usually are modeled by *hard spheres*. Further tests of the MCT for other systems can be found in, e.g., Refs. [4–6]. MCT in its original form describes an idealized glass transition which is indicated by breaking of ergodicity at a critical density ρ_c (or critical temperature T_c). The corresponding nonergodicity parameter $f(\mathbf{q}) = \lim_{t\to\infty} S(\mathbf{q},t)/S(\mathbf{q},0)$ becomes nonzero at ρ_c (or T_c). Recently, the mode coupling equations have been extended to molecular systems. The dynamics of liquids of rigid molecules composed of M atoms can be described by either site-site correlators $S_{\alpha,\beta}$ ($\alpha,\beta = 1,2,\ldots,M$) or molecular correlation functions $S_{lmn,l'm'n'}(\mathbf{q},t)$, where for the latter one decomposes the degrees of freedom into the center of mass and orientational components (see, e.g., [7,8]). The density $\rho(\mathbf{x},\Omega,t)$ is a function of the center of mass coordinate $\mathbf{x}$ and the orientation $\Omega = (\Phi, \theta, \chi)$, which is specified by the three Euler angles. Expanding $\rho(\mathbf{x},\Omega,t)$ with respect to a product basis of plane waves $e^{i\mathbf{q}\cdot\mathbf{x}}$ and generalized spherical harmonics $D_{mn}^l(\Omega)$ one arrives at the tensorial density $\rho_{lmn}(\mathbf{q},t)$. l

runs over all positive integers including zero and m and n take integer values between $-l$ and l. Then the molecular correlators are defined as follows:

$$S_{lmn,l'm'n'}(\mathbf{q},t) = \frac{1}{N} \langle \rho_{lmn}^*(\mathbf{q},t) \rho_{l'm'n'}(\mathbf{q},0) \rangle. \qquad (1)$$

The extension of MCT to molecular systems has been done for the molecular representation for a single dumbbell in a simple, isotropic liquid [9], for molecular liquids of linear molecules [10], and for arbitrarily shaped molecules by use of nonlinear fluctuating hydrodynamics [11] and by the Mori-Zwanzig projection formalism [12]. A MCT approach using a site-site description has recently been worked out [13]. Because a hard ellipsoid corresponds to a rigid body with infinitely many constituents, it is the molecular representation that is the only appropriate one. Since we consider ellipsoids *of revolution* the third Euler angle χ becomes redundant. This means that we have to consider $S_{lm0,l'm'0}(\mathbf{q};t)$ only. Using the $\mathbf{q}$ frame [8], i.e., one chooses $\mathbf{q}=(0,0,q) \equiv \mathbf{q}_0$ where $q=|\mathbf{q}|$, these correlators become real and diagonal in m and m' [10]:

$$S_{lm0,l'm'0}(\mathbf{q},t) = \delta_{m,m'} S_{ll'}(q,m,t). \qquad (2)$$

The head-tail symmetry of the ellipsoids implies that these correlators vanish for $l+l'$ odd. For given X_0 the critical packing fraction $\phi_c(X_0)$ can be determined by calculating the (unnormalized) nonergodicity parameters $F_{ll'}(q,m) = \lim_{t\to\infty} S_{ll'}(q,m;t)$.

II. MOLECULAR MODE-COUPLING EQUATIONS

Using the densities $\rho_{lm}(q,t)$ and longitudinal translational currents $j_{lm}^T(q,t)$ and rotational currents $j_{lm}^R(q,t)$ as the slow variable set for the Mori-Zwanzig projection operator technique, the molecular MCT equations have been derived and can be found in Refs. [10] and [12]. The time dependent molecular MCT equations can be represented as follows:

$$\frac{\partial}{\partial t}\mathbf{S}(q,m,t) = \mathbf{N}^R(q,m,t) + \mathbf{N}^T(q,m,t),$$

$$\frac{\partial}{\partial t}\mathbf{N}^\alpha(q,m,t) = -\boldsymbol{\Omega}_\alpha^2(q,m)\mathbf{S}(q,m,t)$$

$$-\sum_{\alpha'} \nu_{\alpha\alpha'}(q,m)\mathbf{N}^{\alpha'}(q,m,t)$$

$$-\boldsymbol{\Omega}_\alpha^2(q,m)\sum_{\alpha'} \int_0^t \mathbf{m}^{\alpha,\alpha'}(q,m,t-t')$$

$$\times \mathbf{N}^{\alpha'}(q,m,t)dt' \qquad (3)$$

and

$$m_{l,l'}^{\alpha,\alpha'}(q,m,t) = \sum_{\substack{\mathbf{q}_1,\mathbf{q}_2 \\ q=|\mathbf{q}_1+\mathbf{q}_2|}} \sum_{m_1} \sum_{\substack{l_1,l_2 \\ l'_1,l'_2}} V_{l',l'_1,l'_2}^{m,m_1,\alpha,\alpha'}{}_{l,l_1,l_2}(q,q_1,q_2)$$

$$\times S_{l_1,l'_1}(q_1,m_1,t)S_{l_2,l'_2}(q_2,m_2,t). \qquad (4)$$

The indices $\alpha,\alpha' \in \{T,R\}$ refer to either translational or orientational currents. $\mathbf{N}^\alpha(q,m,t)$ are the current-density correlation functions for translational ($\alpha=T$) and rotational ($\alpha=R$) currents multiplied by q and $\sqrt{l(l+1)}$, respectively. The microscopic frequency matrix is denoted by $\boldsymbol{\Omega}_\alpha(q,m)$ and is determined by the static molecular correlators. In the absence of memory effects ($\mathbf{m}^{\alpha,\alpha'}=\mathbf{0}$) the equations are just a set of coupled harmonic oscillators with friction $\nu_{\alpha\alpha'}$ for vibrational ($\alpha=T$) and rotational ($\alpha=R$) oscillations. For example, the translational mode with $l=l'=0$ is the propagating phonon mode and the modes with $l=l'>0$ that exhibit a frequency gap at $q=0$ are *localized* oscillators.

For $\mathbf{m}^{\alpha,\alpha'}\neq\mathbf{0}$ nonlinearities occur. Their physical origin is the memory effect. The corresponding memory kernel is a correlation function of fluctuating forces. Since fluctuating forces can decay into a *pair* of density excitations, this kernel is approximated as a sum of all possible *bilinear* products of density correlation functions. Such a nonlinear feedback mechanism can cause an ideal glass transition with nontrivial dynamics. The glass transition for Eqs. (3) and (4) is investigated in the following part of the paper. The explicit expressions for the vertices $V^{\alpha\alpha'}$ for arbitrary $\mathbf{q}$ can be found in Ref. [10] and for the $\mathbf{q}$ frame in Ref. [12]. The vertices $V^{\alpha\alpha'}$ depend only on the static correlators $S_{ll'}(q,m)$ and the direct correlation function $c_{ll'}(q,m)$, which are related to each other by the Ornstein-Zernike equation. We have determined $c_{ll'}(q,m)$ within the Percus-Yevick approximation.

It has been shown that the liquid phase of hard ellipsoids is well described by these approximations [14]. Although Percus-Yevick theory fails to describe crystallization it yields a nematic instability [14] that is in reasonable agreement with Monte Carlo simulations [15] even if Percus-Yevick theory still underestimates the tendency toward orientational order. This nematic instability will play an important role in the following. For the solution of the Percus-Yevick (PY) equations we have chosen a cutoff $l_{co}=4$ for l and l', whereas the MCT equations were truncated at $l_{co}=2$. We are confident that even such a small number of molecular correlators enables us to capture the correct physics of the transition.

III. SOLUTION OF THE MOLECULAR MCT FOR HARD ELLIPSOIDS

The numerical solution of Eqs. (3) and (4) for $t\to\infty$ yields the nonergodicity parameters $F_{ll'}(q,m)=\mathbf{F}(q,m)$. In the limit of $t\to\infty$ the following set of nonlinear equations for $\mathbf{F}(q,m)$ has to be solved in an iterative way:

$$\sum_{\alpha\alpha'} q_l^\alpha(q)q_{l'}^{\alpha'}(q)[\mathcal{F}(q,m)^{-1}]^{\alpha\alpha'}\mathbf{S}^{-1}(q,m)\mathbf{F}(q,m)$$

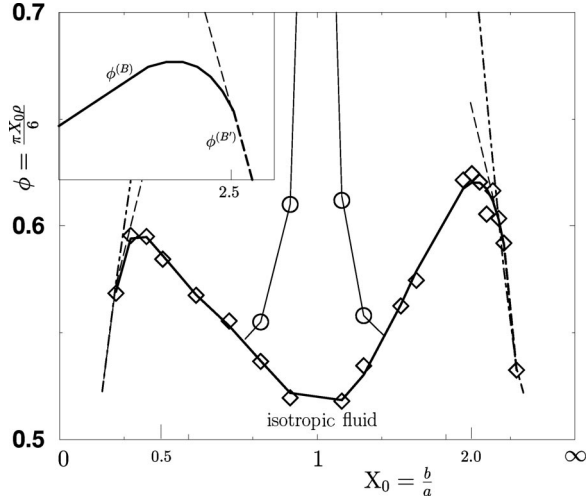$$+\mathbf{F}(q,m)-\mathbf{S}(q,m)=\mathbf{0}, \qquad (5)$$

FIG. 1. Phase diagram for the ideal glass transition. The horizontal axis shows X_0 scaled with $(X_0^2-1)/(X_0^2+1)$. The type-B glass transition lines $\phi_c^B(X_0)$ and $\phi_c^{B'}(X_0)$ (see text) are depicted as thick solid and dashed lines, respectively. The thin solid line is the $\phi_c^{(A)}(X_0)$ glass transition line. The nematic instability occurs at $\phi_{nem}(X_0)$ and is shown as thin dashed-dotted lines. The inset shows the situation around $X_0=2.5$ where the $\phi_c^B(X_0)$ glass transition line merges into the $\phi_c^{B'}(X_0)$ transition line. For $x_0 \geqslant 2.5$ the $\phi_c^{B'}(x_0)$ transition is the physical one (thick dashed line) whereas for $x_0 \leqslant 2.4$ it is an unphysical solution (thin dashed line).

$$\mathcal{F}_{l,l'}^{\alpha,\alpha'}(q,m) = \sum_{\substack{\mathbf{q}_1,\mathbf{q}_2 \\ q=|\mathbf{q}_1+\mathbf{q}_2|}} \sum_{m_1} \sum_{\substack{l_1,l_2 \\ l_1',l_2'}} V_{l',l_1',l_2'}^{m,m_1,\alpha,\alpha'}(q,q_1,q_2)$$

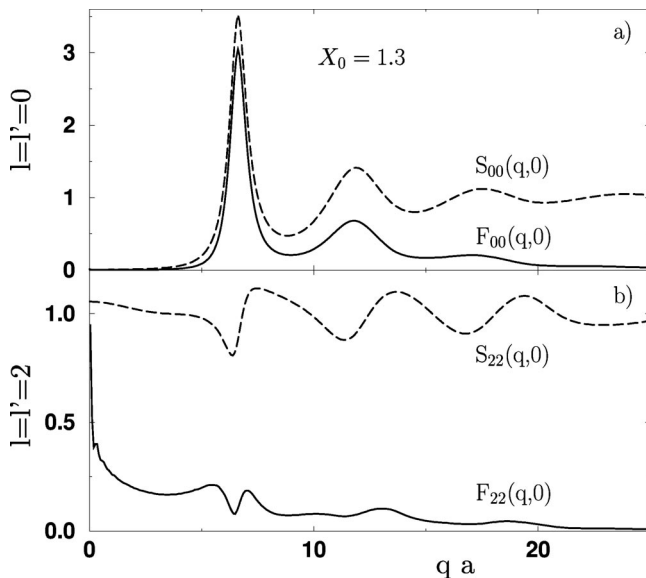$$\times F_{l_1,l_1'}(q_1,m_1) F_{l_2,l_2'}(q_2,m_2), \qquad (6)$$

with

FIG. 2. The static structure factor $S_{ll'}(q,m)$ is plotted together with the nonergodicity parameter $F_{ll'}(q,m)$ for $X_0=1.3$ and $\phi=0.549$ (directly above the nonergodicity transition). (a) shows the center of mass correlator $l=l'=m=0$ whereas (b) shows the quadrupolar correlator $l=l'=2, m=0$.
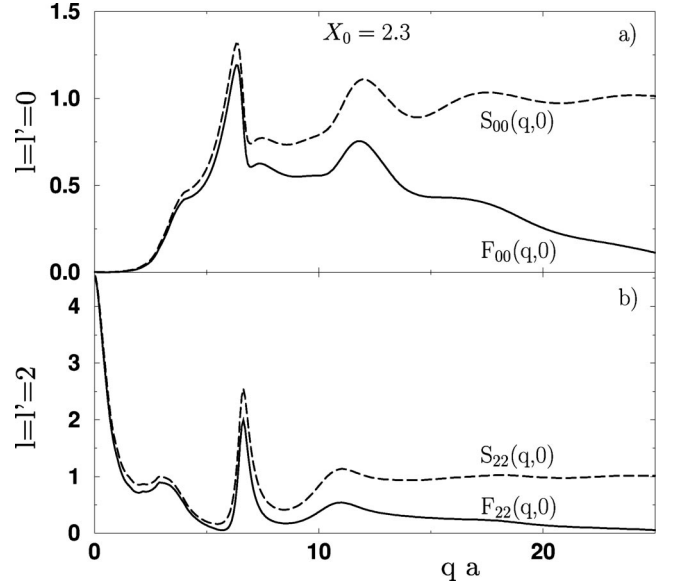

FIG. 3. A similar plot as Fig. 2 is shown but for $X_0=2.3$ and $\phi=0.617$ (again directly above the nonergodicity transition), which is already close to the nematic instability.

$$q_l^\alpha(q) = \begin{cases} q & \text{for} \quad \alpha=T \\ \sqrt{l(l+1)} & \text{for} \quad \alpha=R. \end{cases} \qquad (7)$$

By

$$\mathcal{F}(q,m) = \lim_{z \to 0} -z\mathbf{m}^{\alpha,\alpha'}(q,m,z) = \lim_{t \to \infty} \mathbf{m}^{\alpha,\alpha'}(q,m,t)$$

we denote the long time limit of the memory kernel. From a solution of these equations we obtain the phase diagram for ideal glass transitions that is shown in Fig. 1. This figure also contains two dashed-dotted lines $\Phi_{nem}(X_0)$ indicating the location of the nematic instability as it arises in thermody-
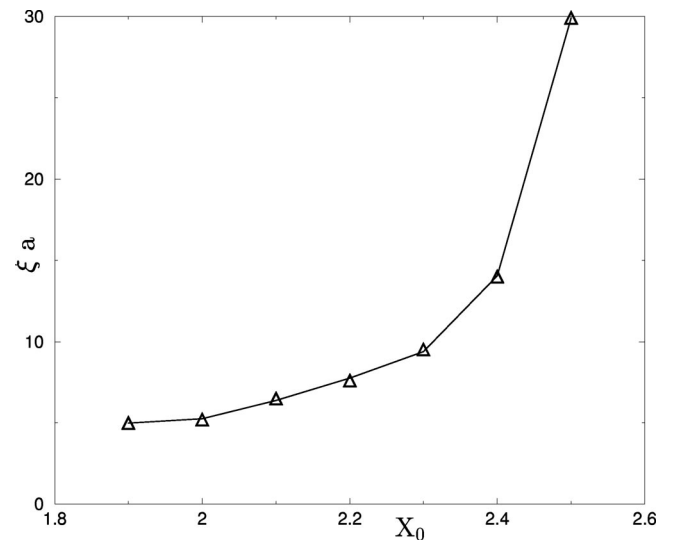

FIG. 4. At the glass transition the correlation length for parallel orientation obtained from the half width at half maximum of the peak of $S_{22}(q,0)$ is plotted as a function of the aspect ratio. For $X_0 \leqslant 2.4$ the glass transition is of type B whereas for $X_0 \geqslant 2.5$ it is of type B' (see text).
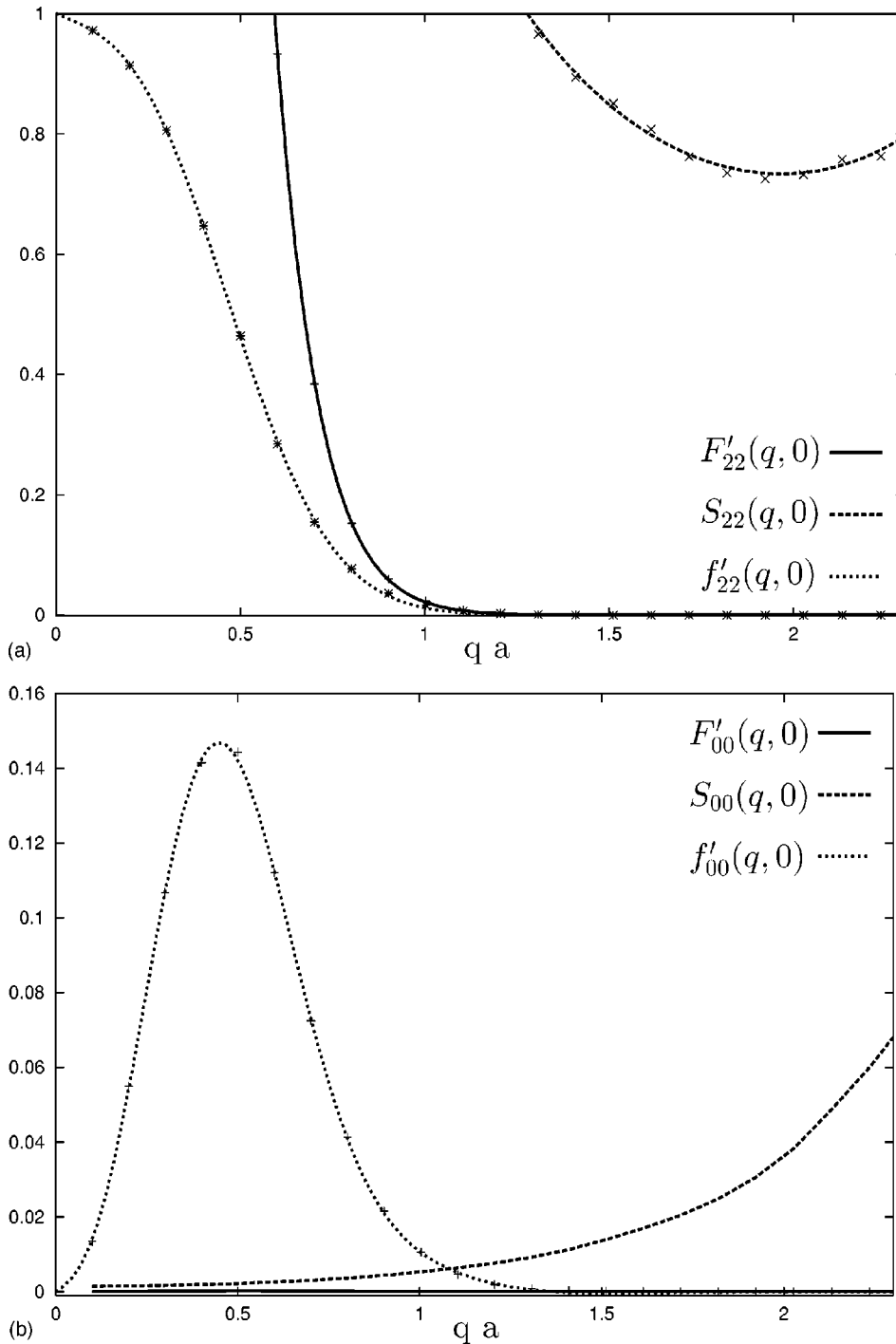
FIG. 5. For $X_0 = 2.5$ and $\phi = 0.593$, the smallest aspect ratio where the type-B' transition occurs, the q dependence of the nonergodicity parameter $F'_{ll'}(q,m)$ is plotted together with the static structure factor $S_{ll'}(q,m)$ and the normalized nonergodicity parameter $f'_{ll'}(q,m) = F'_{ll'}(q,m)/S_{ll'}(q,m)$. In (a) this is done for $l = l' = 2$ and $m = 0$ whereas (b) shows the same quantities for the center of mass $l = l' = m = 0$.

namic equilibrium from PY theory [14]. These two lines are in agreement with density functional theory [16] and Monte Carlo simulations [15]. In addition there are *three* glass transition lines each for $X_0 < 1$ and $X_0 > 1$. First of all we will discuss the critical line $\phi_c^{(B)}(X_0)$ (thick solid line) at which both translational and orientational degrees of freedom for l and l' even undergo a discontinuous ergodic to nonergodic transition (also called the type-B transition). The existence of $\phi_c^{(B)}(X_0)$ has been established for $0.35 < X_0 < 2.5$. In the region where the $\phi_c^{(B)}(X_0)$ glass transition occurs the equilibrium system shows crystallization. Since this is a first order phase transition the onset of crystallization gives two densities (e.g., from Monte Carlo simulations [15]) resulting from

a Maxwell construction. The $\phi_c^{(B)}(X_0)$ glass transition line is well bracketed between these two densities. This indicates that the mode-coupling equations describe a glass transition in the metastable region of a supercooled liquid. The physical origin of the glass transition depends strongly on the location of $\phi_c^{(B)}(X_0)$. For aspect ratios X_0 close to 1 the transition is dominated by the center of mass correlator $S_{00}(q,0)$.

To illustrate this point we have plotted in Fig. 2 the static center of mass correlator and the ''quadrupolar'' correlator $S_{22}(q,0)$ and their corresponding nonergodicity parameters for $X_0 = 1.3$. This was done directly above the critical packing fraction $\phi_c = 0.549$. The first peak at $q_{max} = q \approx 6.6 a^{-1}$
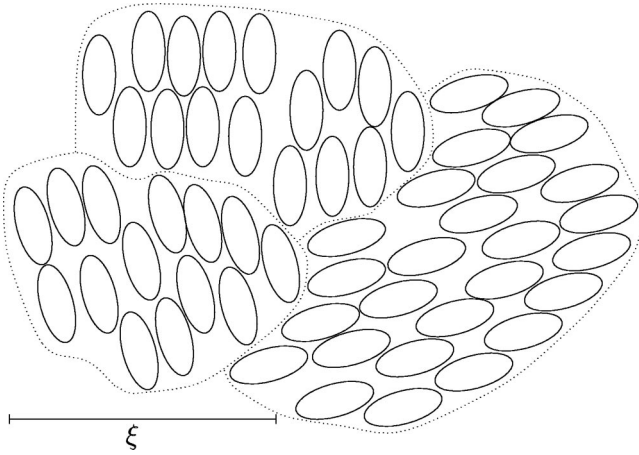
FIG. 6. The formation of the $\phi_c^{(B')}$ glass transition is illustrated. Within each domain of diameter ξ the system shows liquid crystalline order whereas for $l \gg \xi$ there are randomly frozen orientational correlations.

of $S_{00}(q,0)$ dominates the transition; this is the manifestation of the cage effect. Stronger deviations of the ellipsoids from spherical symmetry, however, alter this behavior. This is demonstrated in Fig. 3, where we have plotted the same correlators as in Fig. 2 but for an aspect ratio of $X_0 = 2.3$. Now the peak at $q \approx 0$ of the quadrupolar correlator $S_{22}^0(q,0)$ (which is for $q = 0$ the Kerr constant for nonpolar fluids) dominates the breaking of ergodicity. The half width Δq (at half maximum) of this peak defines a correlation length $\xi = 2\pi/\Delta q$. In Fig. 4 we have plotted ξ at the glass transition line (either $\phi_c^{(B)}$ or $\phi_c^{(B')}$) as a function of the aspect ratio X_0 for prolate ellipsoids.

Within the glassy phase, i.e., for $\phi > \phi_c^{(B)}(X_0)$, a continuous (also called type-A) glass transition occurs at the critical lines $\phi_c^{(A)}(X_0)$ (thin solid lines in Fig. 1) at which the self part of the correlators with l and l' odd freezes. This type-A transition can only occur if the corresponding vertex V is large enough. For this to happen the aspect ratio should clearly be different from 1. The reader should note that four points (open circles in Fig. 1) were determined exactly and the thin solid lines are schematic, showing that $\phi_c^{(A)}(X_0)$ has to increase if X_0 is changed toward 1, in order to keep the vertices large enough. The physical interpretation is that at $\phi_c^{(A)}(X_0)$ the 180° jumps of the ellipsoids become frozen. This resembles the formation of orientational glasses. One possible candidate for such a transition might be plastic crystals like the carboranes [17] although presently only type-B transitions are known.

Probably the most interesting result is the third critical line $\phi_c^{(B')}(X_0)$ (dashed line) which is shown schematically in Fig. 1 for $X_0 > 2.0$ (prolate ellipsoids) and $X_0 < 0.5$ (oblate ellipsoids). In this region the glass transition lines are close to the nematic instability line. The existence of $\phi_c^{(B')}(X_0)$ is based on our following observations. On increasing ϕ for $2.1 < X_0 < 2.5$ we find a glass transition at $\phi_c^{(B)}(X_0)$ where all $F_{ll'}(q,m)$ become nonzero. On increasing ϕ further we find in addition a second solution $F'_{ll'}(q,m)$ for $\phi \gtrsim \phi_c^{(B)}(X_0)$. This solution has the feature that $F'_{ll'}(q,m)$ is essentially zero with the exception of a well pronounced peak for

$F'_{22}(q,m)$ at $q = 0$ and with a width of order ξ. We have shown this in Fig. 5(a), where we have plotted $F'_{22}(q,0)$ at the $\phi_c^{(B')}$ transition for $X_0 = 2.5$. This is plotted together with the static correlator $S_{22}(q,0)$ and the normalized function $f'_{22}(q,0) = F'_{22}(q,0)/S_{22}(q,0)$. In Fig. 5(b) we have plotted the same quantities for $l = l' = 0$; the center of mass correlator. $f'_{00}(q,0)$ does not exceed 0.15 although the orientations are frozen. This means that the system is ''quasiergodic'' in the sense that for length scales $l \ll \xi$ the ellipsoids show a (nematic) orientational order and the center of mass behaves quasiergodically, decaying to a very small value. For length scales $l \gg \xi$, however, the orientations as well as the positions have nondecaying, long-time correlations and are frozen. The easiest way to think of such a system is due to the formation of liquid crystalline (nematic) domains with a size of the order of ξ. This is visualized in Fig. 6. Figure 4 shows that the domains can be quite large. For $X_0 = 2.5$ (the aspect ratio where the type-B' transition occurs first and where therefore the type-B' transition with the smallest domain size shows up) we obtain from our calculation a domain size with $\xi \approx 30$. Within the domains the center of mass is quasiergodic, i.e., liquidlike, whereas the orientations are frozen with a nematic order. In our idealized MCT an ellipsoid cannot move from one domain to the other.

In connection with this it is also interesting to mention that two types of type-B transition were also found for the center of mass correlator of a *simple* liquid of hard spheres with an attractive interaction given by either the Baxter model [18] or a Yukawa potential [19]. The existence of these two solutions for $X_0 > 2.1$ reflects the competition between the frozen positional disorder due to the cage effect and the tendency to form a nematic phase. Since $F'_{ll}(q,m) < F_{ll}(q,m)$ for $2.1 < X_0 < 2.5$, the second solution is unphysical [20]. However, for $X_0 \gtrsim 2.5$ and $\phi_c^{(B')}(X_0) \lesssim \phi \lesssim \phi_{nem}(X_0)$ we find only one solution, which has all the features of $F'_{ll'}(q,m)$ described above. We stress that the existence of the critical line $\phi_c^{(B')}(X_0)$ depends on our choice of slow variables, which include the nematic order parameter, and therefore accounts for the occurrence of the weakly first order nematic transition. Since $\phi_c^{(B')}(X_0)$ is rather close to $\phi_{nem}(X_0)$ quasicritical fluctuations appear, which also slow down the entropy fluctuations. We do not think that these will qualitatively change the phase diagram. On the other hand, the concept of a glass transition induced by the vicinity of a second order phase transition has already been introduced by a MCT approach [21] in order to describe the experimentally observed central peak phenomenon close to a ferroelectric instability.

IV. CONCLUSION

In conclusion, we have shown that hard ellipsoids exhibit a rather intriguing phase diagram obtained from the idealized mode-coupling theory for molecular systems, where the orientational degrees of freedom and their coupling to translational ones are incorporated. In particular, we predict a glass transition for $X_0 > 2$ that is driven by a precursor of a nematic phase. Ellipsoids show two type-B glass transition lines ($\phi_c^{(B)}$ and $\phi_c^{(B')}$). One, $\phi_c^{(B)}$, is dominated by the cage effect whereas the other one, $\phi_c^{(B')}$, is caused by an orienta-

tional (nematic) instability. Besides this a type-A glass transition occurs for almost spherical ellipsoids where the orientational degrees of freedom with odd parity, e.g., 180° flips, freeze independently of the translational ones. It would be very interesting to check these predictions by experiments or simulations.

[1] U. Bengtzelius, W. Götze, and A. Sjölander, J. Phys. C **17**, 5915 (1984).

[2] W. van Megen and S. M. Underwood, Phys. Rev. E **47**, 248 (1993).

[3] M. Fuchs, W. Götze, S. Hildebrand, and A. Latz, Z. Phys. B: Condens. Matter **87**, 43 (1992).

[4] W. Götze, in *Liquids, Freezing and the Glass Transition, Course 5*, edited by J. P. Hansen, D. Levesque, and J. Zinn-Justin (North-Holland, Amsterdam, 1991).

[5] R. Schilling, in *Disorder Effects on Relaxation Processes*, edited by R. Richter and A. Blumen (Springer, Berlin, 1994).

[6] *Proceedings of the Second Workshop on Nonequilibrium Phenomena in Supercooled Fluids, Glasses and Amorphous Materials* [J. Phys.: Condens. Matter **11**, A1 (1999)].

[7] J. P. Hansen and I. R. McDonald, *Theory of Simple Liquids*, 2nd ed. (Academic Press, London, 1986).

[8] C. G. Gray and K. E. Gubbins, *Theory of Molecular Fluids, Volume 1: Fundamentals* (Clarendon, Oxford, 1984).

[9] T. Franosch, M. Fuchs, W. Götze, M. R. Mayr, and A. P. Singh, Phys. Rev. E **56**, 5659 (1997).

[10] R. Schilling and T. Scheidsteger, Phys. Rev. E **56**, 2932 (1997).

[11] K. Kawasaki, Physica A **243**, 25 (1997).

[12] L. Fabbian, A. Latz, R. Schilling, F. Sciortino, P. Tartaglia, and C. Theis, Phys. Rev. E **60**, 5768 (1999); **62**, 2388 (2000).

[13] S.-H. Chong and F. Hirata, Phys. Rev. E **58**, 6188 (1998).

[14] M. Letz and A. Latz, Phys. Rev. E **60**, 5865 (1999).

[15] D. Frenkel, B. M. Mulder, and J. P. McTague, Phys. Rev. Lett. **52**, 287 (1984).

[16] B. Groh and S. Dietrich, Phys. Rev. E **55**, 2892 (1997).

[17] R. Brand, P. Lunkenheimer, U. Schneider, and A. Loidl, Phys. Rev. Lett. **82**, 1951 (1999).

[18] L. Fabbian, W. Götze, F. Sciortino, P. Tartaglia, and F. Thiery, Phys. Rev. E **59**, R1347 (1999).

[19] J. Bergenholtz and M. Fuchs, Phys. Rev. E **59**, 5706 (1999).

[20] It was proved in [4] that the largest solution of the nonlinear MCT equations is the physical one. It is not clear whether this can be extended to molecular liquids. However, we have found that $F'_{ll}(q,m) < F_{ll}(q,m)$ for all q,m and $l=l' \leq 2$, so it is tempting to believe that it is still true.

[21] V. L. Aksienov, M. Bobeth, N. M. Plakida, and J. Schreiber, Z. Phys. B: Condens. Matter **69**, 393 (1987).